

PRINCIPLES OF FLUID DYNAMIC SIMILARITY ANALYSIS FOR SLOSH EXPERIMENTS

Jedediah M. Storey*, Daniel R. Kirk†

Most tank slosh test programs are not conducted with flight hardware in a flight-like environment due to cost and schedule constraints. Instead, subscale tanks are typically tested on the ground. If the “real”, flight liquid in the tank is a cryogenic propellant, sometimes a cryogen is used during testing, but more often a simulant liquid is used. Fluid dynamic similarity analysis, or “scaling analysis” as it is sometimes called, for slosh examines nondimensional numbers to determine which fluid dynamic regime(s) a tank is operating in. If the relevant nondimensional numbers of a scale tank test are similar enough to the real tank’s nondimensional numbers, then it is likely that the scale test data will be similar to what would be obtained with the real tank. This type of analysis is useful for guiding experiment design, test liquid selection, and for understanding the physical relevance of prior test data to a specific application. The authors have performed scaling analyses for many slosh test programs conducted in ground, parabolic flight, suborbital, and in-orbit environments. Basics of how to perform the analysis, along with select examples from ground and microgravity environments, are presented. Suggestions for various assumptions and compromises to make are discussed. Limitations and challenges are also discussed.

INTRODUCTION

Slosh dynamics must be accounted for in the design of control systems for liquid-propelled launch vehicles and spacecraft. Mechanical analogies of slosh, e.g. pendulum, are often used in control simulations and autopilots. The mechanical analogy parameters can be determined from full-scale slosh experiments with flight tanks and propellants, but this is often cost-prohibitive. Even if full-scale slosh testing could be performed, a 1 G acceleration environment may not be characteristic of the flight acceleration environment. Thus, analytical methods and/or simulations of slosh are more commonly used to determine the mechanical analogy parameters^{1,2}. However, the simulations must be validated using physically relevant test data. Subscale slosh testing with propellant simulants is typically less expensive than full-scale slosh testing, so is more common. The test data is used to validate models and/or simulation methodologies, and then the methodologies are used to simulate the full-scale flight tank slosh, the results of which can be used to calculate mechanical analogy parameters for flight.

Numerous subscale ground slosh test campaigns have been conducted, and many of the data from these experiments are available in the literature^{1,3}. These data sets have been used to validate various analytical and CFD methods for a variety of common tank shapes. There are gaps in the available slosh test data, particularly for uncommon tank geometries and reduced-gravity

* Thermal-Fluid Discipline Expert, NASA KSC LSP, Kennedy Space Center, FL.

† Professor, Department of Aerospace, Physics, and Space Sciences, Florida Institute of Technology, Melbourne, FL.

environments, which might drive requirements for slosh testing for some programs. It is assumed that the researcher has determined a need to perform slosh testing. An exhaustive list of available slosh data and the process behind determining the need for slosh testing are out of scope for this paper.

Simulant fluids are used in slosh testing for cost and hazard-reduction reasons, and to help achieve fluid dynamic similarity (discussed in Theory Section) via tailoring of fluid properties. While fluid properties are important, there are practical downsides to using some simulants. As an extreme example, testing with liquid oxygen is more expensive and hazardous than testing with water. If testing with a cryogen is required, liquid nitrogen might be used as a simulant for a cryogenic propellant to mitigate flammability risk. Some simulants have material compatibility problems. For example, solvents should not be used in clear acrylic tanks. Some are environmental hazards. For example, the 3M™ Novec™ and FC engineered fluids contain “forever chemicals” PFAs/PFCs, which are being banned. Hygroscopic liquids can result in property changes over time, which could affect test results. Laboratories often have restrictions on allowable chemicals. Thus, it is necessary to consider all aspects of the fluid for fluid simulant selection. Although an exhaustive list of potential simulant fluids and hazards is out of the scope of this paper, the provided examples discuss simulant selection for their specific applications.

Despite the copious available slosh test campaigns reports, discussions of the basis of the test design are often lacking, and even fewer publications used principles of fluid dynamic similarity, sometimes called “scaling analysis”, to design the tests. This paper attempts to address these shortcomings by presenting the theory of fluid dynamic similarity for tank slosh and applying it to three examples based on real slosh testing campaigns. The authors hope it will be a useful guide for future researchers planning slosh experiments.

THEORY

This section presents the theory of fluid dynamic similarity as it relates to slosh testing. Following the principles of this theory will allow the reader to design slosh experiments that provide test data physically relevant to the desired application.

Nondimensional Numbers

The important variables for isothermal slosh flows are: acceleration, a , characteristic length, L , liquid velocity, U , liquid dynamic viscosity, μ , liquid density, ρ , and surface tension, σ . Acceleration and velocity are dependent on the motion of the tank, L is chosen to be the tank diameter, D , and the others are liquid properties. Finding a set of nondimensional numbers given a list of variables often starts with the Buckingham Pi theorem, however, the relevant nondimensional numbers are already known. The Reynolds number (Re), Weber number (We), and Bond number (Bo) are defined in Eqs. (1)-(3), including the ratio of forces (inertia, viscous, body acceleration, or surface tension) they represent. “Body acceleration” forces are often referred to as “gravity” forces, and “surface tension” forces are sometimes referred to as “capillary” forces. The Froude number (Fr), Capillary number (Ca), and Galileo number (Ga) are defined in Eqs. (4)-(6) and are ratios of the previous three nondimensional numbers.

$$Re = \frac{\text{inertia}}{\text{viscous}} = \frac{\rho LU}{\mu} \quad (1)$$

$$We = \frac{\text{inertia}}{\text{surface tension}} = \frac{\rho LU^2}{\sigma} \quad (2)$$

$$Bo = \frac{\text{body acceleration}}{\text{surface tension}} = \frac{\rho a L^2}{\sigma} \quad (3)$$

$$Fr = \frac{\text{inertia}}{\text{body acceleration}} = \sqrt{\frac{We}{Bo}} = \frac{U}{\sqrt{aL}} \quad (4)$$

$$Ca = \frac{\text{viscous}}{\text{surface tension}} = \frac{We}{Re} = \frac{\mu U}{\sigma} \quad (5)$$

$$Ga = \frac{\text{body acceleration}}{\text{viscous}} = \frac{Bo Re^2}{We} = \frac{\rho^2 a L^3}{\mu^2} \quad (6)$$

Similarity

If all nondimensional numbers can be matched between two different flows, then those flows are fluid dynamically identical. This is ideal because it means that slosh in the (likely subscale) test tank is fluid dynamically identical to slosh in the real tank. Unfortunately, achieving this is rarely possible in practice. Instead, the tests are designed to make the nondimensional numbers as similar as possible between the test and real tanks. If these numbers for the test fall in the same fluid dynamic “regimes” as for the real tank, then the slosh test and its results can be considered fluid dynamically “similar” to slosh in the real tank. Figure 1 depicts three different fluid dynamic regimes based on We and Bo .

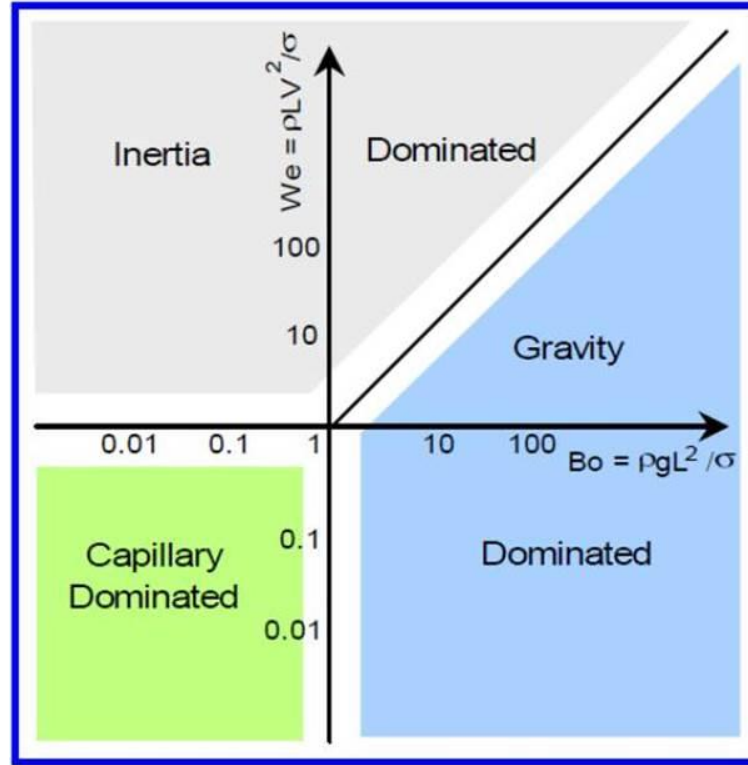


Figure 1. Regimes. (source: Fig. 4.5 from Reference 2)

The diagonal line is $Fr=1$. For both $We \ll 1$ and $Bo \ll 1$, the liquid in the tank is dominated by surface tension, or “capillary”, forces. Inertia forces dominate for $We \gg 1$, and gravity forces

dominate for $Bo \gg 1$. For example, if the slosh test and real tank slosh fall to the far right in Figure 1, then even if the Bo and We are not identical between the test and real tank, the slosh will be body acceleration dominated and behave similarly. The authors' experience with tank slosh testing suggests $Bo \gtrsim 100$ is necessary to avoid the majority of surface tension effects and $Bo \gtrsim 10000$ for them to be negligible. Low We microgravity, i.e. $We < 1, Bo < 1$, slosh is characterized by slow surface waves. Surface tension dominated slosh can be modeled with a mechanical analogy², where the surface tension is modeled as a spring, if the liquid stays in a known configuration. On the other hand, high We microgravity, i.e. $We > 1, Bo < 1$, slosh is often characterized by drops and blobs of liquid moving around the tank. Figures similar to Figure 1 can be generated for other pairs of nondimensional numbers to help visualize different regimes.

Unfortunately, it is difficult to achieve fluid dynamic similarity for all three Bo , We , and Re . Reynolds number is an indicator of laminar versus turbulent boundary layers during sloshing, which affects viscous wall damping and dissipation in tanks. If viscous wall damping is not important or significant, e.g. when baffles are present and dominate slosh damping, then obtaining a similar Re to the real tank in the test is unnecessary. If viscous wall damping is important, but Re matching is not possible, then being squarely in the same Re regime, i.e. laminar or turbulent, for both the test and real tanks is advisable.

Similarity analysis is further complicated by the fact that these nondimensional numbers are unsteady due to the dynamic nature of slosh. Many assumptions are often necessary to make similarity analysis feasible. Examples of possible assumptions include fixed fill level, planar slosh, given wave amplitude, fixed fluid properties, no internal tank features, and constant acceleration. The choice of assumptions is application specific, and all assumptions should be explicitly stated and defended.

Finding a single liquid velocity by relating it to the acceleration environment is often the simplest approach for that variable. Examples 1 and 2 assume planar slosh and relate liquid velocity to body acceleration via maximum slosh wave speed. Example 3 assumes orbital maneuvers drive bulk motion of the liquid, so liquid velocity is related to the maneuver acceleration.

Non-isothermal Slosh

More variables, and therefore more nondimensional numbers, are relevant if thermodynamics are of concern. The isothermal assumption is sufficient for storable propellants, e.g. RP1, but thermodynamics may need to be considered for sloshing of cryogenic liquids, particularly when the effects of slosh on the ullage are important. Achieving fluid *and* thermodynamic similarity can be extremely difficult for cryogenic slosh, and using a cryogen as the test fluid, e.g. LN₂, is often necessary. An in-depth discussion of thermodynamic similarity is out of the scope of this paper.

Fluid Properties

Fluid properties can be obtained from sources such as NIST⁴, REFPROP⁵, and CoolProp⁶. Care should be taken when selecting properties of cryogens; ensure that the operational temperature and pressure conditions are considered.

Theory Summary

In summary, a slosh test needs to be fluid dynamically similar to slosh in the real tank to generate physically relevant test data, which can then be used to validate analytical/numerical slosh methods. Fluid dynamic similarity is achieved by designing the test such that the slosh in both the test and real tanks is in the same nondimensional number regimes. The following three sections provide examples based on real slosh testing campaigns.

EXAMPLE 1: LAUNCH VEHICLE TANK GROUND SLOSH TESTING

Background and Setup

This example is based on a ground slosh test campaign of scaled launch vehicle cryogenic propellant tanks. Slosh testing was determined to be necessary for multiple reasons: 1. To validate the analytical/numerical methods for calculating mechanical analogy parameters by finding them empirically for subscale tanks in 1 G, 2. To generate physically relevant test data for validating slosh CFD, 3. Unique/nonstandard tank geometry, 4. An interest in accurate characterization of nonlinear damping. There is also a requirement to visually record the slosh tests, meaning the test tanks must be transparent. Specifics have been modified/obfuscated for this paper to protect proprietary information.

For this example, it is assumed that there are two linear stage test facilities available. The first is a countertop linear stage that can handle up to 25 cm diameter tanks. The second is a large linear stage that can handle tanks up to several tons and 1.25 m in diameter. A picture of one of FloridaTech's large linear stages is shown in Figure 2 for reference.

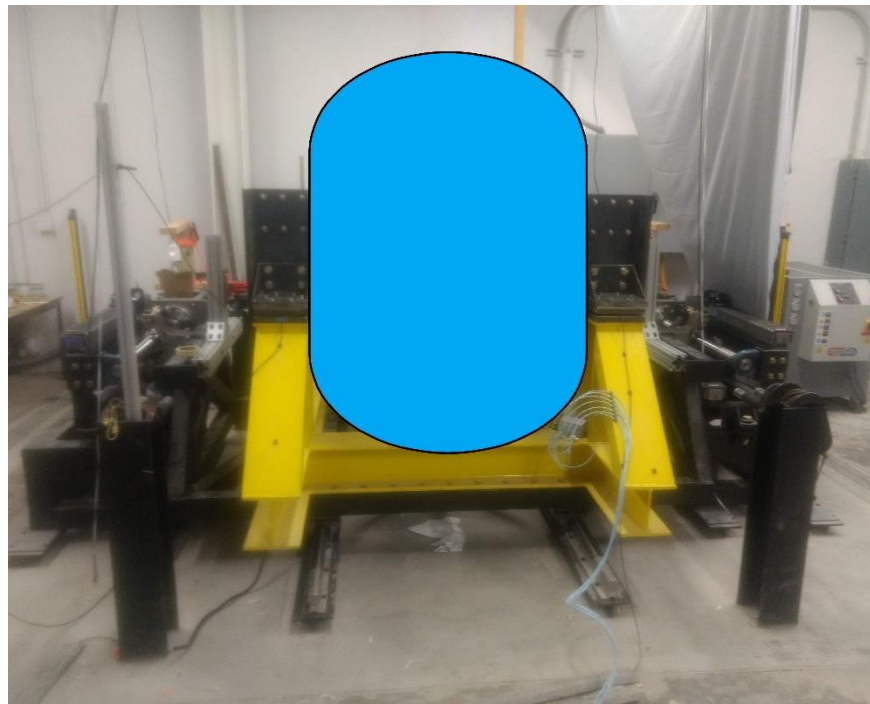


Figure 2. FloridaTech Large Linear Stage 1.

The linear stages have three high-load triaxial force sensors, which enable measurement of 3-axis slosh forces and moments. Measuring forces, moments, and slosh angle, as well as proper test selection, allows for collecting data that can be used to calculate all first slosh mode mechanical analogy parameters, except fixed mass inertia, which requires pitching the tank.

Analysis

Fluid dynamic similarity analysis is used to choose the scale of the test tanks and the test fluid. The goal is to design the slosh tests to obtain nondimensional numbers in the test tanks similar to those in the full-scale tanks with propellants, meaning the slosh dynamics would be similar. The real tanks have the same diameter, 5 m, but different geometry; despite this, it is assumed they can all be approximated as cylinders, meaning this analysis only needs to be performed for one real

tank. If that was not the case, then this analysis would need to be repeated for the other geometry, e.g. spherical. Utilizing the maximum capacities of the linear stages (to make Bo and We as close to the real tanks under flight-like acceleration as possible) yields two test tank scales, either 1/20 or 1/4. The tanks are assumed to have a quiescent fill height of 1 radius from the bottom. The slosh wave amplitude is fixed at 1/10th of the diameter. Despite baffles being present in the real tanks, and eventually present in the test tanks, the tanks are assumed to have smooth walls for this analysis. The presence of an aft dome and ring baffle(s) will influence the first mode frequency, but ignoring these effects is assumed to be acceptable for this analysis. Scale testing is done on the ground (1 G). The real tanks are analyzed over a range of accelerations. The real propellants are LH₂ and LO₂ and are assumed to be at their normal boiling points (NBPs). The simulant fluids 3M Novec 7100, mineral oil, water, are at standard temperature and pressure (STP). LN₂ at its NBP is also considered as a simulant fluid.

The first asymmetric slosh mode frequency of a cylinder is calculated analytically using Eq. (7).

$$\omega_1 = \sqrt{\left[\frac{a\xi_{mn}}{R} + \frac{\sigma\xi_{mn}^3}{\rho R^3} \right] \tanh\left(\frac{\xi_{mn}h}{R}\right)}, \quad (7)^7$$

where ξ_{mn} is a constant dependent on wave number (1.841 for first asymmetric mode), R is tank radius, ω is frequency in rad/s, and h is fluid height. Eq. (7) includes a surface tension correction, but that term is negligible at high accelerations. Frequency can be used to estimate the maximum slosh wave velocity at the fluid surface:

$$U = U_{max} = \omega_1 z, \quad (8)$$

where z is the wave amplitude (assumed to be 1/10*D).

Table 1 shows Re at 1 G for the different tanks and fluids.

Table 1. Example 1 Reynolds Numbers.

Scale	Fluid	Re
full	LH ₂	3.4E7
full	LO ₂	3.8E7
1/4	Novec 7100	2.1E6
1/4	Mineral oil	6.8E3
1/4	Water	9.2E5
1/4	LN ₂	4.1E6
1/20	Novec 7100	1.9E5
1/20	Mineral oil	608
1/20	Water	8.2E4
1/20	LN ₂	3.7E5

Ideally, test tank Re would be as close to that of the real tanks as possible to make smooth wall viscous damping similar. The Re for the 1/20 scale tank with water is a factor of 460 smaller than Re for the full-scale LO₂ tank. Like the full-scale tank Re 's, the 1/4 scale tank Re 's, except mineral oil, are $> 5E5$, so the wall boundary layer is likely in the turbulent regime for some of a slosh cycle.

None of the 1/20 scale tank Re 's are $> 5E5$, so the wall boundary layer is likely laminar for the whole slosh cycle. For tanks with baffles installed (with fluid height above the baffle), the baffle pressure drag dominates the wall boundary layer viscous damping, so attempting to match Re is not as important for those tests.

Figure 3 shows We versus Bo for the scale tanks with a few select simulants at 1 G and the real tank with the two propellants over accelerations 0.0001 - 2 G. Only the endpoints of the curves are marked ('+') for the propellants.

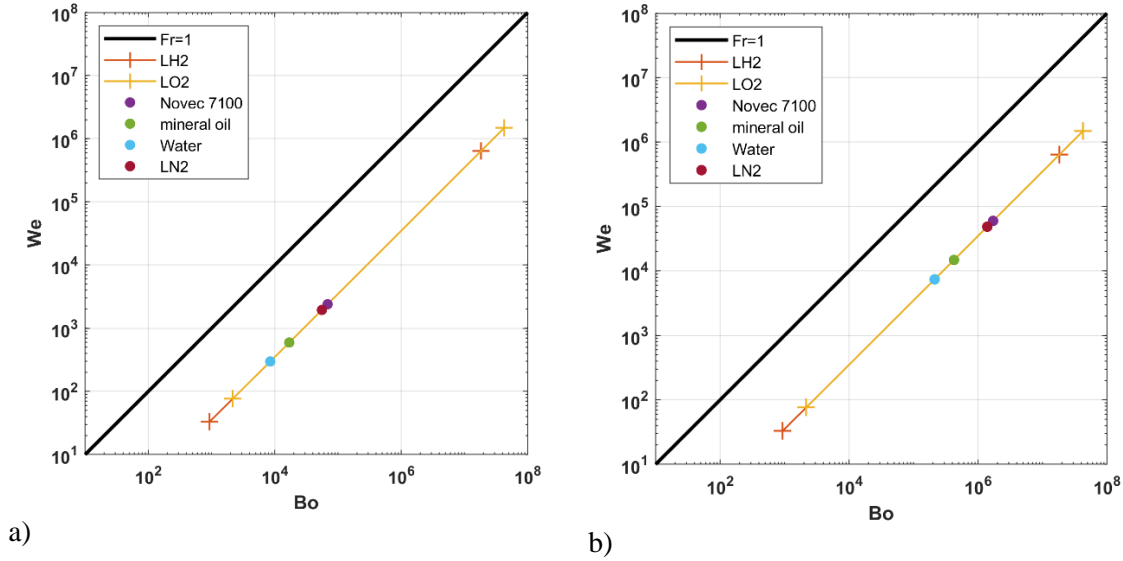


Figure 3. We vs. Bo : a) 1/20 scale, b) 1/4 scale.

All calculated points have $Fr \approx 0.187$ due to a , U , and L being related by Eq. (8), meaning the slosh is in the body-acceleration-dominated regime. Different values of Fr will result from different choices of wave amplitude. Water and mineral oil Bo 's for the 1/20 scale tank are borderline too low. Novec is expensive, far too expensive to fill the 1/4 scale tank, though a possibly acceptable expense for the 1/20 scale tank. LN_2 results in similar We and Bo numbers to Novec while being less expensive. However, the LN_2 would likely cause thermal stress cracking in an acrylic tank, which, due to the transparent tank requirement, would necessitate the use of a glass cryostat and negate the cost benefit of using LN_2 over Novec. If matching thermodynamic nondimensional numbers were of interest, then LN_2 and a custom glass cryostat might be worth pursuing. Interestingly, the 1/4 scale tank with water results in higher We and Bo than any of the fluids in the 1/20 scale tank, which highlights the advantages of large-scale slosh testing. Slosh in the 1/4 scale tank with water in 1 G will be similar to the full-scale tank with LH_2 at an acceleration of 3.6 m/s^2 and with LO_2 at an acceleration of 1.5 m/s^2 ; these accelerations are below flight accelerations, but can still be considered “high-G”.

Example 1 Summary

Mineral oil should be excluded based on Re due to interest in characterizing damping. 1/20 scale test tanks on the small linear stage with Novec 7100 would likely be the most economical option that could yield useful results, but if budget allows, 1/4 scale tanks with water would be better.

This only looked at linear, asymmetric slosh mode excitation. Exciting rotary modes is possible with linear excitation. It is also possible to perform rotational slosh testing with appropriate test facilities, e.g. the Spinning Slosh Test Rig (SSTR, formerly at SwRI now at FloridaTech).

EXAMPLE 2: PARABOLIC FLIGHT AIRCRAFT SLOSH TESTING

Background

This example is based on a parabolic flight experiment that tested a capacitive gauging system in a tank partially filled with liquid⁸. The test tank was spherical, approximately 0.175m diameter, and was a subscale representation of a launch vehicle upper stage cryogenic propellant tank. Different fill levels were tested on different flights, and the unsteadiness of the low gravity portions of the parabolas drove slosh. The study had a strict schedule and relatively low budget.

Analysis

Because the tank had been fabricated prior to the start of the experiment campaign, adjusting/selecting the test hardware was not possible. Thus, fluid dynamic similarity analysis informed the test fluid selection, i.e. selecting μ , ρ , and σ to achieve We and Bo ranges as close to that of a real tank as possible. Obtaining fluid dynamic similarity ensured realistic unsettled fluid configurations in the test tank during the parabolic flights. Of course, arbitrary selections of fluid properties are not possible, and, due to the capacitive gauging system, this experiment had another driving requirement for a test fluid with low relative permittivity, as close to that of cryogenics ($\approx 1.2 - 1.6$) as possible.

Testing with a cryogen would have been ideal. Although cryogenics can be flown on research parabolic flights, cost constraints precluded their use in this experiment. Specifically, the time and cost of tank modifications, and the cost of the ground handling equipment and LN₂ Dewar rentals, made it infeasible. All non-toxic and non-flammable 3MTM NovecTM and FC engineered fluids, as well as some common fluids like mineral oil and distilled water, were surveyed to compile a list of candidate simulants. As mentioned previously, engineered fluids offer wide ranges and combinations of μ , ρ , and σ (and other properties) at the expense of cost. Most engineered fluids are non-toxic, but they sometimes have environmental concerns. For example, the 3MTM NovecTM and FC fluids are PFAs/PFCs (“forever chemicals”), but this experiment was performed prior to their ban.

The full-scale, “real” tank was assumed to be a 3 m diameter sphere with no internal features and 50% filled with either LO₂, LH₂, or LCH₄ as the sloshing fluid. The cryogenics in the real tank were assumed to be at their NBPs, and the simulant fluids were at STP. Using more realistic operational temperature and pressure for the cryogenics would have been more accurate, but NBPs were sufficient for this study. Thermodynamic effects, e.g. boiling, were ignored. Characteristic length was assumed to be tank diameter. The net acceleration environment of the parabolas ranged from approximately 0 to 20 m/s². Planar slosh was used to relate acceleration to the maximum slosh wave speed, and wave amplitude was assumed to be 1/10th of the tank diameter. Unlike Example 1, the low gravity environment means that surface tension effects on slosh need to be considered.

The first asymmetric slosh mode frequency of a spherical tank does not have a simple analytical solution. Reference 9 tabulates the slosh frequency parameter for various wave numbers and modes versus fill level. For 50% fill fraction and first mode:

$$\lambda = \frac{\omega^2 R}{a} = 1.56, \text{ for } \frac{h}{2R} = 0.5, \quad (9)$$

where λ is the nondimensional frequency parameter, R is tank radius, and ω is frequency in rad/s, and h is fill height. Eq. (9) assumes no surface tension forces, the inclusion of which makes Eq. (9) dependent on contact angle. Figure 4.20 of Reference 2 plots the first and second asymmetric slosh modes’ frequency parameter in a spherical tank assuming a 0 deg contact angle (perfectly wetting). For cryogenics, 0 deg contact angle is generally a good assumption, but it is a poor

assumption for water. That plot was tabularized (taking into account radius versus diameter), the above $\lambda = 1.56$ asymptote from Eq. (9) added in, and Figure 4 was created.

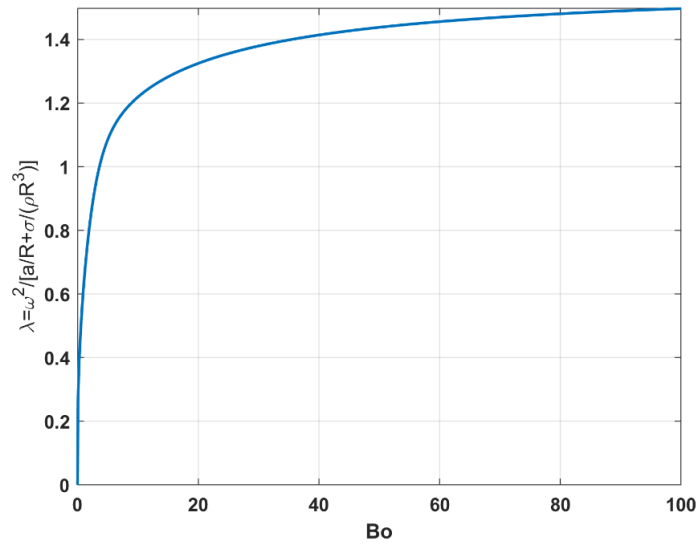


Figure 4. Frequency Parameter vs. Bond Number for $h/2R=0.5$.

The frequency parameter asymptotes to 1.56 at high Bond number ($\lambda \approx 1.56, Bo \gtrsim 100$), as expected. Frequency can be used to estimate the maximum slosh wave velocity at the fluid surface using Eq. (8). Zero acceleration (true 0 gravity) results in a frequency and velocity of 0.

We , Bo , and Re were calculated over a scale test acceleration range of 0.0001-20 m/s^2 . The acceleration experienced by some launch vehicle upper stages during attitude control maneuvers is on the order of 0.0001 m/s^2 , so this is used as a lower limit for convenience. Figure 5 plots We versus Bo for the scale tank with a few select simulants over accelerations 0.0001-20 m/s^2 and the real tank with the three cryogenics over accelerations 0.0001-1 m/s^2 . Only the endpoints of the curves are marked: 'o' for simulants and '+' for cryogenics.

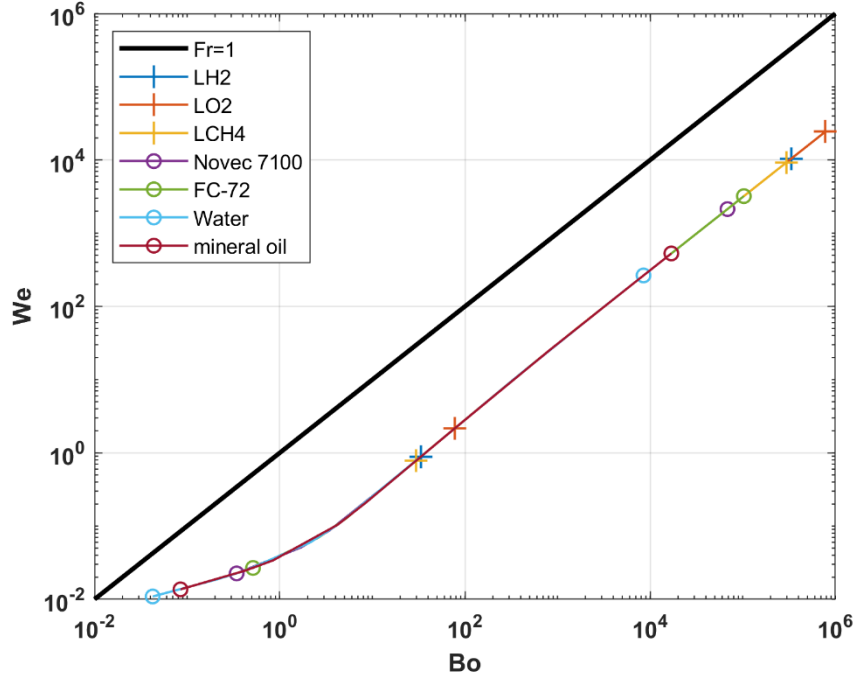


Figure 5. Example 2 We vs. Bo.

All of the simulants achieved $Bo < 1$ at the low end of the acceleration range, so surface tension effects should be observable during the low-G portions of the parabolas. For high Bo , $Fr \approx 0.177$, but Fr drops at low Bo due to surface tension modifying the first mode frequency. Different values of Fr will result from different choices of wave amplitude. Water had the lowest Bo and We of the simulants considered, resulting in the least overlap with the cryogenics. That, in addition to its relative permittivity being the highest of the simulants, made water a poor choice for this study. 3M FC-72¹⁰ achieved the highest Bo and We of the simulants, resulting in the most overlap with the cryogenics. A way to interpret these results is the scale test tank with FC-72 on the parabolic flight was fluid dynamically similar to the real tank with cryogenics in an acceleration environment of near 0 m/s² to about 0.15 m/s². For this analysis, Re in the real tank was 70-180 times larger than in the test tank with FC-72, so viscous damping was not expected to be similar. This was considered acceptable for this study because slosh damping similarity and characterization was not an objective. That said, FC-72 was better than many of the other simulants surveyed in this respect. For example, mineral oil Re was about 300 times lower than FC-72 Re . Finally, FC-72 also had the lowest relative permittivity of the candidate simulants, so it was selected as the test fluid.

Example 2 Summary and Comments

The fluid dynamic similarity analysis resulted in FC-72 being selected as the simulant fluid. During the flights, Bo ranged from near 0 to approximately 100,000 and We from near 0 to approximately 3,000.

FC-72 had a high vapor pressure, so ground handling equipment was designed to prevent as much evaporation as possible within cost constraints. Material compatibility was checked. The high vapor pressure required accounting for mass transfer to/from the ullage gas (air-vapor) mixture, an additional post-processing complication. Because FC-72 was expensive, the exact quantity required was purchased, and the subsequent ban made obtaining more impossible, so ground handling procedures were more strenuous than would have been required with something like water.

EXAMPLE 3

Background and Setup

The ISS SPHERES-Slosh Experiment (SSE) Program studied the behavior of liquid motion within a tank under long-term microgravity conditions¹¹. The primary objective of the SSE program was to collect high-resolution imagery of long-duration, low-gravity, coupled-motion slosh with synchronized motion data and well-defined initial conditions. The end goal was a dataset useful for validating microgravity slosh CFD simulations¹².

The “long-duration, low-gravity” aspects meant the experiment would have to be done in space. Utilizing the ISS Laboratory was significantly less expensive than a bespoke satellite, and utilizing existing hardware already on the ISS, the Synchronized Position Hold Engage Reorient Experimental Satellites (SPHERES) robots, reduced costs and enabled rapid development. The test tank was sized based on the capabilities of the SPHERES thrusters. ISS payload requirements documents and regulations drove many of the design decisions.

For this program, “long” duration slosh is defined as similar duration to on-orbit spacecraft maneuvers, which typically last between several seconds to several minutes. On-orbit maneuvers of launch vehicle upper stages were used to inform the selection of maneuvers the SSE would perform and to determine relevant accelerations for input to a nondimensional scaling analysis.

To prevent vapor pull-through and gas ingestion into the rocket engine, propellant settling maneuvers typically use reaction or attitude control thrusters to apply a small acceleration to settle the liquid propellant at the sump of the tank. Passive thermal control (PTC) maneuvers are rotations about a stage’s primary acceleration axis (roll) during long coasts that distribute solar heating around the stage’s tanks, preventing hot spots. An attitude change maneuver reorients the stage to point in a specific direction and sometimes involves both a translation and a rotation. Attitude change maneuvers are performed for various reasons, such as orienting a stage for a main engine burn or spacecraft separation event. Tank dimensions, thrusts, time durations, accelerations, rotation rates, and angular accelerations for these maneuvers were selected from publicly available data for a variety of launch vehicles.

To ensure fluid dynamic similarity between actual spacecraft and the SSE, relevant nondimensional numbers were matched (where possible) between the full-scale upper stages and the SSE’s initial tank designs and maneuvers. Ideally, this analysis would also inform the selection of the test fluid, however due to ISS regulations, permissible test fluids were limited and distilled water was selected. As the analysis and trade studies progressed, it became clear that the largest tank that the SPHERES could feasibly move would be necessary. The final tank was a pill shaped, 150mm in diameter, with hemispherical ends. Therefore, the fluid dynamic similarity analysis primarily informed the maneuvers to perform, instead of tank geometry or fluid selection as in the previous examples.

Since accurate measurement of viscous damping was not a primary objective of the SSE, *Re* similarity was not necessary, though viscosity was relevant to PTC maneuver analysis (discussed shortly). Relevant scale velocity and acceleration needed to be derived for each maneuver type to examine *Bo* and *We*.

Settling Maneuver

It is assumed that the initial velocity of the liquid relative to a stationary pill-shaped tank is zero, and the initial collated liquid location is at one end of the tank. For the actual SSE experiments, it is recognized that these initial conditions are difficult to attain. Further, it is known that even small variations in initial conditions can lead to different fluid dynamic behaviors for the same motion.

For the purposes of the scaling analysis, the tank is accelerated at an acceleration, a , towards end of the tank that initially held the liquid. In the reference frame of the tank, this results in the liquid traversing the major axis of the tank for an assumed distance of $2R$, and impacting the tank wall with a final velocity, U . Eq. (10) is used to compute final velocity.

$$U^2 - 0 = 2a2R \rightarrow U = \sqrt{4aR} \quad (10)$$

We and Bo were calculated for all tanks for various a , the results of which are plotted in Figure 6. The “water” points are from the SSE.

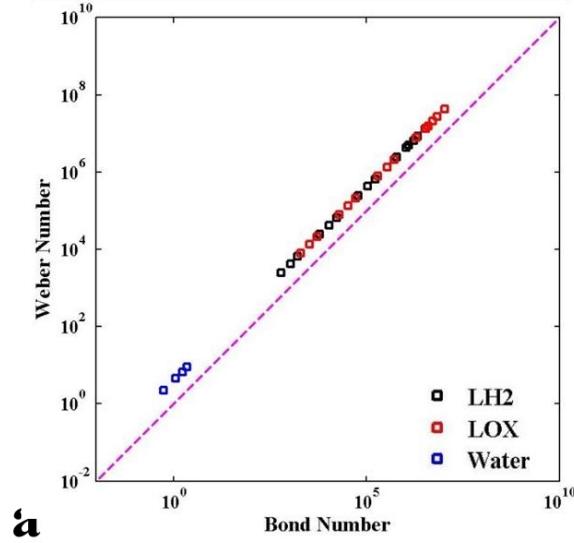


Figure 6. We vs Bo, Settling Maneuver.

The dashed line represents $Fr=1$. All calculated points have $Fr=4$ due to a , U , and L being related by Eq. (10), which means the rocket upper stage and SSE tanks are slightly in the inertia-dominated regime for this maneuver. Neither Bo nor We could be matched with water as the SSE test fluid. Matching We and/or Bo would require a larger tank and a simulant liquid with a larger ρ/σ ratio. Larger a , resulting in larger U , can partially compensate, however, acceleration is ultimately limited by the thrust performance of the SPHERES, or ISS crewmembers if maneuvered manually.

Passive Thermal Control Maneuver

PTC maneuver scaling was accomplished by adjusting the rotation rate of the SSE tank about its major axis to obtain similar We and Bo as full-size upper stage vehicles. The smaller radius of the SSE tank meant that the rotation rate of the SSE had to be higher to produce the required centripetal acceleration and velocity at the tank wall consistent with full-scale vehicles. The rotating tank wall accelerates adjacent liquid due to viscous drag, and centripetal acceleration causes the liquid to collect on the tank wall. Eventually, the liquid achieves a steady state condition similar to solid body rotation. The amount of time it takes for this condition to develop is related to the momentum diffusion length scale. The solution to the Navier-Stokes equation for impulsively started flat plate at constant speed, which can be used as an analog to the case of a rotating tank if curvature effects are ignored, results in $\delta \propto \sqrt{\nu t}$, where ν is kinematic viscosity, and t is time. This can be used to estimate the required SSE (r)evolution time as follows:

$$\frac{\delta_{fs}/R_{fs}}{\delta_{SSE}/R_{SSE}} = 1 = \frac{\sqrt{v_{fs}t_{fs}}}{\sqrt{v_{SSE}t_{SSE}}} \rightarrow t_{SSE} = \frac{v_{fs}}{v_{water}} t_{fs} \quad (11)$$

where the subscript fs denotes one of the full-scale tanks. For example, the ratio $\frac{v_{fs}}{v_{water}}$ for LH₂ is approximately 0.21, meaning the SSE tank takes about 1/5 as long as a LH₂ tank to reach a similar rotating fluid state. This assumes no radial baffles, stringers, isogrid, or other internal tank structure that could enhance the liquid's rotation, are in the tank, which is the case for the SSE tank (smooth walls), but is not the case many examples of actual upper stage tanks, which means Eq. (11) t_{SSE} is an overestimate. The fact that $t_{SSE} < t_{fs}$ is convenient because it means the simulated PTC maneuver performed with the SSE can be shorter than with a full-scale tank.

An ISS safety requirement limited the rotation rate (axial roll) of the SSE to 60 deg/s. Despite this limitation, *We* and *Bo* similarity were achievable for this maneuver.

Attitude Change Maneuver

The attitude change maneuver consists of both a translation and rotation, and the rotation is about an axis other than the tank-axial/roll axis. Tank dimensions, maneuver time, and degrees rotated set the angular and linear accelerations and velocities, which are used to calculate *We* and *Bo*. Similar to the PTC maneuver, the rotation rate can be adjusted to achieve *We* and *Bo* similarity between the SSE and full-scale tanks. However, the rotation rate was limited to 10 deg/s due to an ISS safety requirement, which is lower than the axial roll rate limit because the SSE sweeps a larger area when rotated about a non-roll axis.

Example 3 Summary and Comments

Water was selected as the test fluid for the SSE due to ISS operational and safety requirements. In summary, the scaled maneuvers resulted in the SSE tank operating in either inertia or acceleration dominated regimes. *Re* similarity was not achieved for the proposed ISS experiments. Exact *Bo* and *We* similarity was not achievable for the scaled settling maneuvers, but similitude was achievable for the PTC and attitude change maneuvers. Additionally, the capillary dominated regime ($Bo < 1$, $We < 1$) was achievable by keeping the acceleration, and resulting fluid velocity, low, i.e. by performing low acceleration, slow maneuvers that generally resulted in surface waves with no bulk fluid motion.

While only alluded to here, ISS regulations are stringent, particularly for free-flying experiments. The slosh researcher should have a general understanding of these regulations before pitching and designing an ISS experiment.

Although surface tension has been incorporated into the analysis, contact angle has not been mentioned yet. Cryogenics have low contact angles on metals, i.e. they are wetting. This was not a problem for Example 2 because the simulant was wetting, but the contact angle of water on the SSE tank material was around 60 deg. Fortunately, this was wetting enough for a fluid film to still form on the tank walls at low *Bo*, but some aspects of the slosh were likely unrealistic due to the contact angle being too large. While the SSE was intended to be similar to launch vehicle upper stage cryogenic tanks, it is possible that some test cases were more representative of storable propellant tanks in spacecraft due to the relatively small test tank and use of water as the test fluid. Contact angle should be understood or characterized prior to low-gravity slosh experiments.

SUMMARY AND FINAL COMMENTS

The theory of fluid dynamic similarity analysis for slosh testing was presented, along with three examples. The first example's fluid dynamic similarity analysis guided selection of a simulant fluid and subscale tank size for ground slosh testing of launch vehicle propellant tanks. The second example's guided selection of a simulant fluid for a low-gravity parabolic flight tank sensor experiment. The third example's guided tank sizing and maneuver selection for an ISS slosh experiment. Slosh test design is somewhat of an art, and the authors hope that this paper helped demystify some of it. A summary of the process of fluid dynamic similarity analysis is as follows:

1. Determine the need for slosh testing.
2. Understand all requirements related to slosh for the application. As every example showed, slosh tests cannot be designed in isolation. Other requirements and drivers often must be considered.
3. Determine which nondimensional numbers are relevant to your application.
4. Determine which "knobs" are available to turn in the design of the slosh test. Examples: fluid, tank size, gravity environment, maneuvers.
5. List all analysis assumptions.
6. Design the test to achieve fluid dynamic similarity between the test tank slosh and slosh in the "real" tank(s).
7. Execute experiment.
8. Check the data. Make sure nondimensional numbers are as expected and that fluid dynamic similarity was achieved.

The majority of launch vehicle and spacecraft mass is often a liquid propellant. Slosh is a chaotic and dynamic process; characterizing and understanding it is critical to mission success. There is a balance between reducing risk upfront with slosh testing and analysis, and gathering flight data, which is (obviously) more useful. Relying on large dispersions, stability margins, and control authority can help accelerate the path to flight. Once flight data has been gathered, it should be thoroughly compared to slosh inputs, and anything unexpected should be investigated.

ACKNOWLEDGMENTS

Within the NASA Launch Services Program, the authors would like to thank Dr. Paul Schallhorn, Brandon Marsell, Jacob Roth, Michael Elmore, and Scott Clark for their contributions to some of the experiments mentioned herein. At FloridaTech, the authors would like to acknowledge Dr. Hector Gutierrez and the many graduate student alumni of the ASAP laboratory for their contributions to various slosh test programs.

REFERENCES

- 1 N. H. Abramson, "The Dynamic Behavior of Liquids in Moving Containers," NASA, Washington, D.C, 1966.
- 2 F. T. Dodge, "The New 'Dynamic Behavior Of Liquids in Moving Containers'," SWRI, San Antonio, Texas, 2000.
- 3 J. M. Storey, "Experimental, Numerical, and Analytical Slosh Dynamics of Water and Liquid Nitrogen in a Spherical Tank," Florida Institute of Technology, Melbourne, FL. <https://repository.fit.edu/etd/514/>, 2016.

- 4 P. Linstrom and W. Mallard, NIST Chemistry WebBook, NIST Standard Reference Database Number 69, Gaithersburg MD, 20899: National Institute of Standards and Technology, 2024.
- 5 E. Lemmon, I. Bell, M. Huber and M. McLinden, "NIST Standard Reference Database 23: Reference Fluid Thermodynamic and Transport Properties-REFPROP, Version 10.0," National Institute of Standards and Technology, Standard Reference Data Program, Gaithersburg, 2018.
- 6 I. Bell, J. Wronski, S. Quoilin and V. Lemort, "Pure and Pseudo-pure Fluid Thermophysical Property Evaluation and the Open-Source Thermophysical Property Library CoolProp," *Industrial & Engineering Chemistry Research*, vol. 53, no. 6, pp. 2498-2508, 2014.
- 7 R. Ibrahim, *Liquid Sloshing Dynamics Theory and Applications*, New York: Cambridge University Press, 2005.
- 8 J. Storey, B. Marsell, M. Elmore and S. Clark, "Propellant Mass Gauging in Microgravity with Electrical Capacitance Tomography," *NASA TP-20230012805*, <https://ntrs.nasa.gov/citations/20230012805>.
- 9 P. McIver, "Sloshing Frequencies for Cylindrical and Spherical Containers Filled to an Arbitrary Depth," *Journal of Fluid Mechanics*, vol. 201, pp. 243-257, 1989.
- 10 3M, *3M Fluorinert Electronic Liquid FC-72 Technical Datasheet*, 2019.
- 11 S. Chintalapati, C. Holicker, R. Schulman, E. Contreras, H. Gutierrez and D. Kirk, "Design of an Experimental Platform for Acquisition of Liquid Slosh Data aboard the International Space Station," in *48th AIAA/ASME/SAE/ASEE Joint Propulsion Conference, AIAA 2012-4297*, Atlanta, GA, 2012.
- 12 J. Storey, "Experiments and Simulations of Liquid Mass Gauging and Slosh Dynamics in Microgravity, Dissertation," Florida Institute of Technology, Melbourne, FL, 2023.